

BLUE COMPACT DWARF GALAXIES WITH NITROGEN OVERABUNDANCE

A view from integral field spectroscopy

Enrique Pérez-Montero (1), José M. Vilchez (1), Bernabé Cedrés (1), Guillermo F. Hägele (2), Mercedes Mollá (3), Rubén García-Benito (4), Ángeles I. Díaz (2), Carolina Kehrig (5), David Martín-Gordón (1)

(1) Instituto de Astrofísica de Andalucía – CSIC. (2) Dpto. de Física Teórica de la Universidad Autónoma de Madrid. (3) CIEMAT, (4) Kavli Institute for Astronomy and Astrophysics, Beijing, China, (5), Astrophysikalisches Institut Postdam, Germany

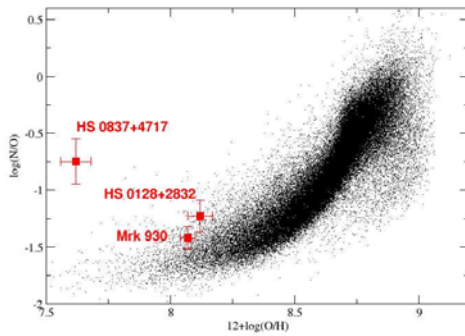
Abstract

Blue compact dwarf galaxies (BCDs) take up the low end of the distribution of metallicity and nitrogen-to-oxygen (N/O) ratio as derived using collisional emission lines in ionized gaseous nebulae. This chemical state is well explained by chemical evolution models. Nevertheless, there is a subsample of BCDs with large values of N/O which cannot be explained by these models. In this poster we present Potsdam Multi Aperture Spectrograph (PMAS) integral field spectroscopy (IFS) of a sample of three of these objects. Our aim is to study the spatial distribution of the physical conditions and chemical abundances, and try to link their spatial variations with possible causes of the local enrichment of their interstellar medium (ISM).

Introduction

The low metallicity regime in the O/H vs. N/O plot is characterized by a "plateau" up to $12+\log(\text{O}/\text{H}) = 8.2$, which is interpreted in terms of a predominant production of primary nitrogen. However, some BCDs present higher values of N/O than expected for their metal content. Between the causes of this offset, it has been proposed: uncertainties in the primary and secondary production of N by low and intermediate-mass stars, outflows of enriched gas by super-massive galactic winds, inflows of metal-poor gas or N pollution of the ISM by Wolf-Rayet (WR) stars.

Integral Field Units (IFUs) are suitable tools to explore the N pollution because they allow to measure the total WR emission in relation with its corresponding gas emission, locating the position of WR stars.



PMAS observing programme

Three BCDs showing N overabundance were observed during one night in October 2008 with the PMAS/IFU mounted at the 3.5 m telescope at the Calar Alto Observatory. In two out of the three BCDs, WR stars were detected previously via long-slit spectroscopy (see Table below).

The figure above shows the O/H and N/O ratios for both the three observed galaxies and all star forming galaxies from SDSS7 catalogue. The abundances of these galaxies were estimated using empirical parameters based on [NII], [OII], H α and H β emission lines.

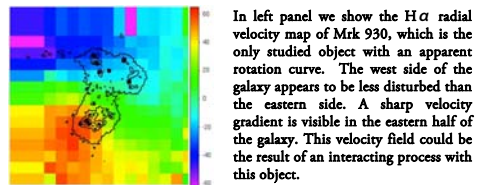
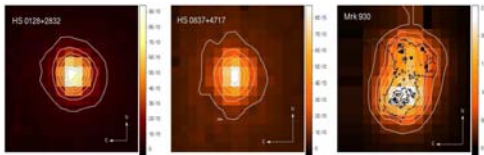
Object name	$12+\log(\text{O}/\text{H})$	$\log(\text{N}/\text{O})$	WR	t_{exp} (s)	Long slit ref.
HS 0128+0832	8.12	-1.23	NO	3900	<i>Isotov & Thuan (2004)</i>
HS 0837+4717	7.62	-0.75	YES	3300	<i>Pustilnik et al. (2004)</i>
Mrk 930	8.07	-1.42	YES	2400	<i>Isotov & Thuan (1998)</i>

The observations were carried out using the Lens Array mode of the PMAS instrument with magnification of $1'' \times 1''$. Therefore the field of view of all images is $16'' \times 16''$. We used the grating V600 in 2×2 binning mode ($1.7 \text{ \AA}/\text{pix}$) to cover from 3600 Å up to 6900 Å in two spectral ranges. The objects were observed at air masses lower than 1.25 to avoid major differential atmospheric refraction effects. Average seeing during the observing night was $2''$.

Reduction was performed using the standard procedures and using the R3D and IRAF packages. Emission line maps were obtained by fitting automatically in each spaxel a gaussian profile around the local continuum. The uncertainty associated to the shape of the fitted gaussian and the position of the continuum were propagated to each derived quantity from these emission line fluxes.

H α maps, morphology and kinematics

Dereddened, continuum subtracted H α maps indicate different morphologies for the three observed objects. In HS0128 and HS0837, the emission structure is quite compact with a prominent central starburst, although at different spatial scale lengths (HS012: 330 pc $''$; HS0837: 840 pc $''$ at the adopted distances). The figures below show the H α emission line maps with the isocontours corresponding to 0.1 fractions of the peak of emission. No apparent kinematical structure is detected in these two objects. Regarding Mrk 930 (380 pc $''$), the isocontours correspond to its HST-ACS image in the UV (F140-LP filter) which better traces the position of the massive ionizing stellar clusters. This galaxy presents a more elongated shape with the brightest knot in the south and other two fainter in the north. Guseva et al. (2000) detected WR emission in the southern knot.

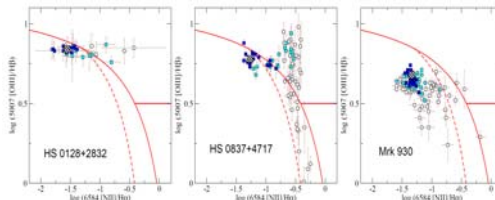


In left panel we show the H α radial velocity map of Mrk 930, which is the only studied object with an apparent rotation curve. The west side of the galaxy appears to be less disturbed than the eastern side. A sharp velocity gradient is visible in the eastern half of the galaxy. This velocity field could be the result of an interacting process with this object.

Diagnostic diagrams based on [NII] lines

The panels below show [NII]H α vs. [OIII]/H β for each one of the individual spaxels in our BCDs. This diagram can be used to distinguish between a pure stellar ionization source (left below the solid and dashed red lines) and active galactic nuclei (AGN; right over the same lines; Baldwin, Phillips & Terlevich, 1981). The points have different colours as a function of their position in relation to the H α maximum: dark blue (with more than a 25% of $F(\text{H}\alpha)_{\text{max}}$), light blue (with $25\% > F(\text{H}\alpha)_{\text{max}} > 12.5\%$) and white ($F(\text{H}\alpha)_{\text{max}} < 12.5\%$). The larger square represents the value that corresponds to the integrated spectrum of each galaxy.

As we see, the integrated points and those with brightest H α emission lie in the star-forming region. However a large fraction in the outer parts of the three galaxies lie in the AGN zone. This is motivated by the ionization structure of the galaxies, with a high emission of the [NII] lines even at large distances from the ionizing source.



Statistical analysis of the distributions

Two main approaches are valid to study the distribution of the physical conditions and chemical abundances of the gas:

1) Integrated. The addition of the flux from all spaxels. It can be used to compare the results of the IFS with those from e.g. long-slit.

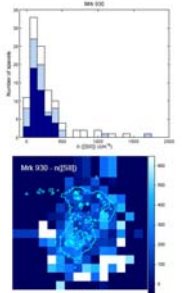
2) Statistical distributions (adopted in this work). It considers all spaxels with the same weight. In these distributions we have applied a Lilliefors test, which fits a gaussian with a determined confidence level. Our starting assumption is to consider as uniform (i.e. the fluctuations have only a statistical origin) those distributions which can be fitted by a gaussian with a confidence level > 10%. This means that for the distributions that pass this test the assumption of homogeneity across the PMAS field of view cannot be rejected.

For all studied cases, the value obtained from the integrated spectrum matches with the average value of the fitted gaussian in those cases where this could not be rejected.

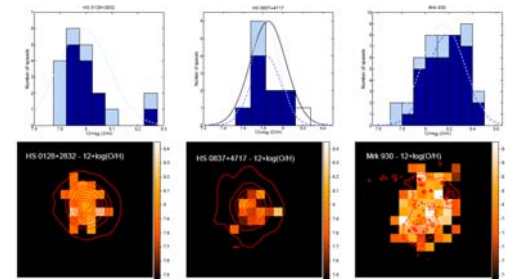
Physical conditions and chemical abundances

Using the emission line maps and only considering the fluxes with S/N > 5, we created the reddening (from the Balmer decrement), excitation (from the [OII]/[OIII] ratio) and the [OIII] electron temperature maps. In general, we find homogeneous distributions in HS0837 and Mrk 930 but, on the contrary, no gaussians are fitted for any of the studied distributions in HS0128.

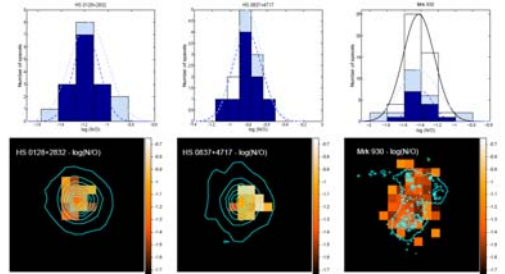
The only exception to an homogeneous behaviour in Mrk 930 appears in the distribution of the electron density measured from the [SII] emission lines. A high density front is visible in the southern region of the galaxy. Therefore, the average values from the three regions are larger than the value measured in the integrated spectrum of the northern knots (32 particles/cm 3). On the contrary the mean values of the distributions are respectively 100, 200 and 290 particles per cm 3 for the inner region (dark blue bars), the intermediate region (light blue bars) and the outer region (white bars)



The [OIII] temperature maps can be used to derive the low excitation temperature using photoionization models (e.g. Pérez-Montero & Díaz, 2003) and derive the O $^+$ and O $^{2+}$ ionic abundances following the direct method and, hence, the O/H total abundance. As in the case of the electron temperature, the abundance is homogeneous in all regions of HS0837 and Mrk930, but this is not the case in HS0128. However, if we make the same analysis using an empirical parameter (e.g. R23, Pagel et al., 1979), we are able to fit a gaussian to the distribution of O/H in this galaxy. So perhaps there is an effect of lack of sampling in the collected temperatures of this galaxy.



Contrary to O/H, the distribution of the N/O ratio in all studied regions of the three galaxies can be fitted by gaussians. This behaviour is also found for the most part of the distributions when we make the same analysis using an empirical parameter (e.g. N2O2, Pérez-Montero & Contini, 2009).



Conclusions

We have presented a PMAS study of three BCDs with low O/H and high N/O. Although the WR bump has been reported in two of the galaxies, this has not been detected in any of our spectra.

The H α maps and kinematics of the gas show that only in Mrk 930, a rotation curve can be fitted. This curve along with the density map of Mrk930, indicates a possible interaction scenario in this galaxy.

The statistical analysis of the spatial distribution of the physical conditions and chemical abundances shows that the most of the distributions can be considered as uniform in the PMAS field of view. In the case of the N/O ratio, this is remarkable because the involved spatial scale lengths and the derived masses of the ionizing stellar clusters preserve the WR stars detected in long-slit observations to be the main cause of the pollution of the ISM in these objects.